



Binary and Ternary Fragmentation Analysis of ^{252}Cf Nucleus using Different Nuclear Radii

Nitin Sharma^{*} and Manoj K. Sharma

Thapar Institute of Engineering & Technology, Patiala, Punjab-147004, India

*nitinsharma2295@gmail.com (Corresponding Author)

ARTICLE INFORMATION

Received: January 19, 2021
Accepted: April 19, 2021
Published Online: August 31, 2021

Keywords:

Ternary fission, Fragmentation potential,
Spontaneous fission



DOI: [10.15415/jnp.2021.91010](https://doi.org/10.15415/jnp.2021.91010)

ABSTRACT

Pioneering study reveals that a radioactive nucleus may split into two or three fragments and the phenomena are known as binary fission and ternary fission respectively. In order to understand the nuclear stability and related structure aspects, it is of huge interest to explore the fragmentation behavior of a radioactive nucleus in binary and ternary decay modes. In view of this, Binary and ternary fission analysis of ^{252}Cf nucleus is carried out using quantum mechanical fragmentation theory (QMFT). The nuclear potential and Coulomb potential are estimated using different versions of radius vector. The fragmentation structure is found to be independent to the choice of fragment radius for binary as well as ternary decay paths. The deformation effect is included up to quadrupole (β_2) with optimum cold orientations and their influence is explored within binary splitting mode. Moreover, the most probable fission channels explore the role of magic shell effects in binary and ternary fission modes.

1. Introduction

Radioactivity is one of the prominent branch of the nuclear physics, which provides opportunity to understand the inter-nuclear forces and related structural aspects. Radioactive decay modes mainly rely on the nuclear stability, shape and size etc. Generally, radioactivity includes various emission mode such as alpha decay, cluster emission, heavy particle radioactivity (HPR) and spontaneous fission (SF). Beside the above-mentioned binary decay modes, a radioactive parent nucleus may also proceed via simultaneous emission of three fragments. This kind of splitting mode is known as the ternary fission. Numerous attempts have been made theoretically as well as experimentally to explore the possible decay modes in the ternary fission [1–4]. For example, a light mass fragment (α particle) may be observed along with two heavier fragments and the process is known as particle accompanied fission. In spite of this, other decay mode is also possible where all of the three decaying fragments are of comparable masses and the process is termed as true ternary fission (TTF). TTF mode is not observed experimentally but some theoretical attempts were made [5–7]. The literature reveals that [8], there are two probable configuration modes in the ternary fission process i.e., equatorial mode and collinear mode. The geometrical mode where the

third fragment emission happens orthogonal to fission axis is known as equatorial mode and when the emission of third fragment happens along the fission axis it is termed as collinear decay mode. Ternary fission is possible mainly in heavy actinides and in super heavy elements. Spontaneous ternary fission (Ground state) was observed experimentally for ^{252}Cf nucleus and relative fragmentation yield was given, with ^4He as the third fragment [9]. In 2010, Yu. V. Pyaktov et al. [10] worked on ^{252}Cf nucleus and proposed ^{48}Ca as the third fragment within collinear configuration mode. In view of above, a theoretical analysis of related aspects is carried out by taking ^{48}Ca as the third fragment by using three cluster model (TCM) [4] and probable decay path is explored using three body penetration profile [1]. Three cluster model is based on the quantum mechanical fragmentation theory (QMFT) [11, 12], which works in terms of mass asymmetry and relative separation coordinates. It is expected that inter-fragment radius plays an important role in the splitting of a radioactive nucleus. Therefore, it would be interesting to analyze the role of different form of fragment radius in binary and ternary fission modes. In view of above, present work aims to analyze the role of inter-fragment radius in binary and ternary decay path of ^{252}Cf radioactive nucleus.

The primary goal of the present work is to explore the fragmentation potential in binary and ternary decay modes

and to observe the behavior of fragmentation structure and barrier characteristics with respect to different choices of inter-fragment radius expressions.

2. Methodology

Binary and ternary fission analysis of ^{252}Cf nucleus is carried out by using the quantum mechanical fragmentation theory (QMFT) [1,4,11,12]. This methodology is worked out in terms of collective coordinates of mass (and charge) asymmetry

$$\eta_A = (A_1 - A_2) / (A_1 + A_2) \quad (1)$$

and relative separation R between the decaying fragments. Here, 1 and 2 represent the heavy and light fragments, and in case of ternary fission, third fragment is kept fixed (represented by A_3). The collective fragmentation potential is given as [1]

$$V = \sum_i \sum_{j>i} B_i + V_{cij} + V_{pij} \quad (2)$$

where the first term B_i represents the binding energy of the decaying fragments i.e. the collective addition of macroscopic liquid drop model and shell corrections taken from the reference [13,14], V_{cij} denotes the Coulomb potential and V_{pij} is the nuclear attractive proximity potential which is given as

$$V_p(S) = 4\pi\bar{R}\gamma b\phi(S) \quad (3)$$

Here S denotes the surface separation of fragments, γ is the surface energy constant, b denotes the surface thickness, R is the mean curvature radius and ϕ the universal function, for detail see the reference [15]. The fragment radius expressions used in present work are taken from [16-18] and read as

$$R_i = 1.28A_i^{1/3} - 0.76 + 0.8A_i^{1/3} \quad (4)$$

$$R_i = C_i + (N_i / A_i)t_i \quad (5)$$

$$R_i = 1.20A_i^{1/3} - 0.09 \quad (6)$$

$$R_i(\alpha_i) = (1.20A_i^{1/3} - 0.09) \left[1 + \sum_{\lambda} \beta_{\lambda} Y_{\lambda}^0(\alpha_i) \right] \quad (7)$$

Among two ternary fission configurations (as discussed in previous section), present work include the collinear configuration [8] mode. The surface separation among three fragments can be taken as $S_{13} = R_1 + R_3 + 2R_2 + 2S$, $S_{12} = R_1 + R_2 + S$, $S_{23} = R_2 + R_3 + S$, where R_1 , R_2 , R_3 are the radius of three fragments and S_{12} , S_{23} , S_{13} represent the relative separation among the three decaying fragments [8], with common separation parameter S . The scattering potential is estimated in terms of Coulomb and proximity potential. The deformation dependent radius vector are also included using eq. (7), for more details, see ref. [19, 20].

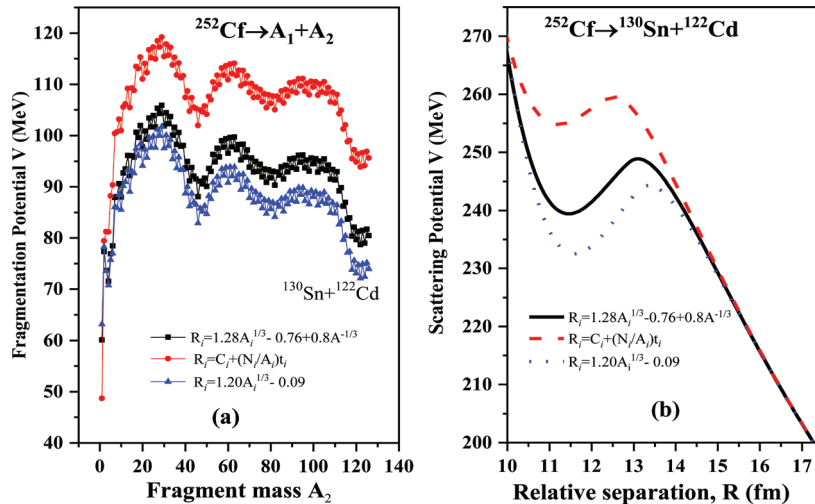


Figure 1: (a) Binary fragmentation potential calculated for ^{252}Cf nucleus using different radius choices. (b) Scattering potential for decay of $^{252}\text{Cf} \rightarrow ^{130}\text{Sn} + ^{122}\text{Cd}$ as a function of inter-fragment radius.

3. Calculations and Discussions

This section represents the theoretical description of binary and ternary fission of ^{252}Cf radioactive nucleus. Initially, the binary fragmentation behaviour is analysed using different

radius expressions (eq. (4), (5), (6)). The fragmentation potential is plotted with respect to the fragment mass A_2 in Fig. 1(a). The calculations are performed using spherical choice of decaying fragments. The minima's in the fragmentation potential represent the dominance of

a particular decay channel with respect to other probable modes. It can be noted from the figure that there is no change in the fragmentation structure with change in the radii expression, but we find significant difference in the magnitude of the fragmentation potential. The binary fragmentation profile suggests that $^{122}\text{Cd}+^{130}\text{Sn}$ is most probable spontaneous fission channel which seems to be triggered via shell closure effect ($Z=50$). The emergence of $^{122}\text{Cd}+^{130}\text{Sn}$ persists independent of the choice of radius vector. Furthermore, magnitude of fragmentation potential is lowest for eq. (6) which means the preformation

probability may be higher with this expression. Now, after the analysis of fragmentation behaviour, total scattering potential is estimated for $^{122}\text{Cd}+^{130}\text{Sn}$ channel to get some idea about the penetration probability for this channel. Figure 1 (b) displays the scattering potential with respect to inter-fragment separation R . It is evident from the figure that barrier position and barrier height change with respect to change in the radius vector, and hence the penetration probability get affected accordingly. In present case, barrier height is observed lowest for $^{122}\text{Cd}+^{130}\text{Sn}$ channel and hence may lead to higher magnitude of penetration probability.

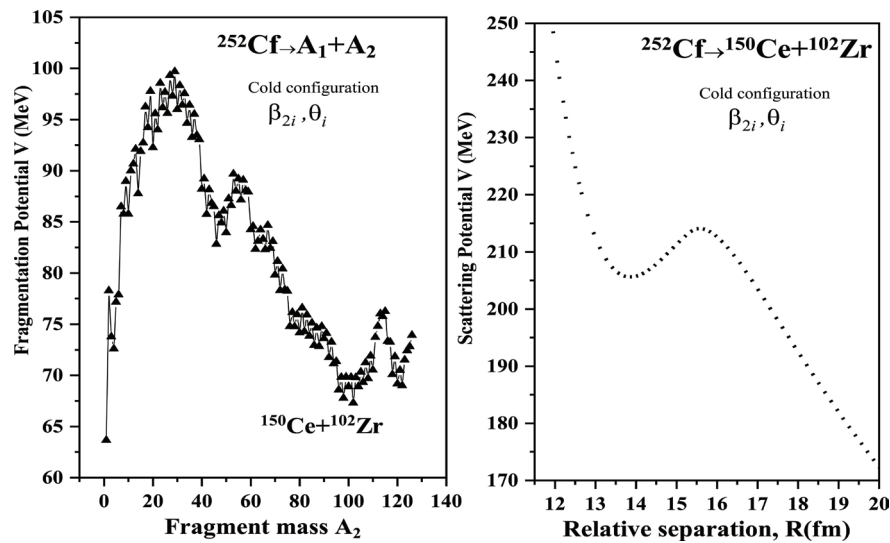


Figure 2: (a) Binary fragmentation potential calculated for ^{252}Cf nucleus using deformed choice of radius. (b) Scattering potential for decay of $^{252}\text{Cf} \rightarrow ^{130}\text{Sn}+^{122}\text{Cd}$ as a function of relative separation (for cold orientation).

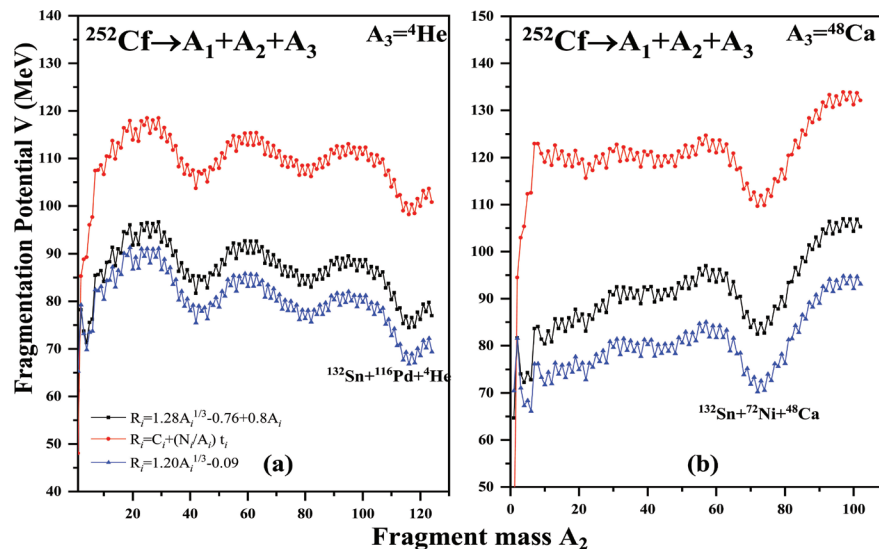


Figure 3: Ternary fragmentation potential is calculated for ^{252}Cf nucleus for (a) light third fragment ($A_3=^4\text{He}$) and (b) heavy third fragment ($A_3=^{48}\text{Ca}$) using different radius expression.

Further, an effort is made to see the impact of deformation dependent radius in the decay dynamics of ^{252}Cf parent nucleus. The deformation effects are included using eq. (7) in view of radius expression shown by eq. (6) as the fragmentation potential is recorded lowest for this choice of radius vector (see Fig. 1 (a)). The fragmentation potential and scattering potential under the influence of deformation effect is shown in Fig. 2. Here Fig. 2 (a) and (b) represent the fragmentation potential and scattering potential for deformed choice of nuclear radius. A significant change is observed in the magnitude of both fragmentation potential calculated for spherical and deformed choice of fragments. A symmetric mass distribution is shown by spherical approach, however, the contribution of symmetric and asymmetric fission fragments is observed for deformed approach. The most probable fission fragment channel changed from $^{122}\text{Cd}+^{130}\text{Sn}$ to $^{150}\text{Ce}+^{102}\text{Zr}$ due to deformed shell effects ($N=62$). The barrier characteristics get significantly modified; the barrier height decreases and barrier position increases after inclusion of deformation effects.

After analysing the binary fragmentation phenomenon, three body fragmentation potential is calculated for light ($A_3=^4\text{He}$) and heavy third fragment ($A_3=^{48}\text{Ca}$) as shown in Fig. 3 (a) and 2 (b). It is evident from the figures that fragmentation structure is independent of choices of the fragment radius (similar to the case of binary fission). Using different radius vectors, same fission channels (i.e., $^{132}\text{Sn}+^{116}\text{Pd}+^4\text{He}$ for light third fragment and $^{132}\text{Sn}+^{72}\text{Ni}+^{48}\text{Ca}$ in case of heavy third fragment) are found, and the role of shell closure is evident. The use of eq. (6) for radius expression, gives lowest fragmentation potential for both cases (light and heavy third fragment), which means that the ternary fragment emission probability may be higher for the use of this expression. Furthermore, the interaction potential for both the channels is plotted with respect to surface separation S , and plotted in Fig. 4 (a) and (b). The barrier height with eq. (6) is lowest and hence may contribute higher penetration probability for suggested ternary fission channels.

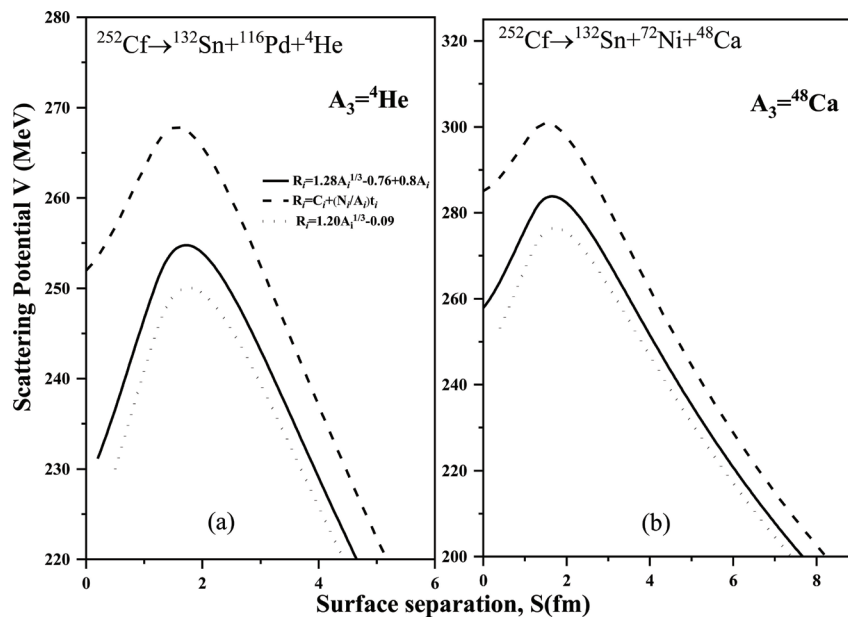


Figure 4: Ternary fragmentation potential is calculated for ^{252}Cf nucleus for (a) light third fragment ($A_3=^4\text{He}$) and (b) heavy third fragment ($A_3=^{48}\text{Ca}$) using different radius expression.

Summary

Summarizing, Quantum mechanical fragmentation theory (QMFT) is used to study the binary and ternary fission of ^{252}Cf radioactive nucleus. The fragmentation behaviour of ^{252}Cf nucleus is calculated for both binary and ternary fission processes by using various choices of fragment radius. It is observed that there is no change in the fragmentation structure with use of different fragment radius expressions.

The most probable binary and ternary fission channels depict the role of shell closure effects. Apart from this, barrier characteristics are estimated for binary and ternary splitting modes. Additionally, influence of deformation dependent radius vector is explored in binary decay mode. It will be of further interest estimate the fragmentation yield for both binary and ternary fission processes.

Acknowledgements

Financial support from the UGC-DAE Consortium for Scientific Research, File No. UGC-DAE-CSR-KC/CRS/19/NP09/0920, is gratefully acknowledged.

Reference

- [1] N. Sharma, A. Kaur and M. K. Sharma, Phys. Rev. C **102**, 064603 (2020).
<https://doi.org/10.1103/PhysRevC.102.064603>
- [2] G. Farwell, E. Segrè and C. Wiegand, Phys. Rev. **71**, 327 (1947). <https://doi.org/10.1103/PhysRev.71.327>
- [3] A. V. Ramayya et al., Phys. Rev. Lett. **81**, 947 (1998).
<https://doi.org/10.1103/PhysRevLett.81.947>
- [4] K. Manimaran and M. Balasubramaniam, Phys. Rev. C **79**, 024610 (2009).
<https://doi.org/10.1103/PhysRevC.79.024610>
- [5] K. R. Vijayraghvan, M. Balasubramaniam and W. von Oertzen, Phys. Rev. C **91**, 044616 (2015).
<https://doi.org/10.1103/PhysRevC.91.044616>
- [6] V. I. Zagrebaev, A. V. Karpov and Walter Griener, Phys. Rev. C **81**, 044608 (2010).
<https://doi.org/10.1103/PhysRevC.81.044608>
- [7] R. B. Tashkodjaev et al., Phys. Rev. C **91**, 054612 (2015).
<https://doi.org/10.1103/PhysRevC.91.054612>
- [8] K. Manimaran and M. Balasubramaniam, Phys. Rev. C **83**, 034609 (2011).
<https://doi.org/10.1103/PhysRevC.83.034609>
- [9] A. V. Ramayya et al., Phys. Rev. C **57**, 2370 (1998).
<https://doi.org/10.1103/PhysRevC.57.2370>
- [10] Y. V. Pyaktov et al., Eur. Phys. J. A **45**, 29 (2010).
<https://doi.org/10.1140/epja/i2010-10988-8>
- [11] J. Maruhn and W. Greiner, Phys. Rev. Lett. **32**, 548 (1974). <https://doi.org/10.1103/PhysRevLett.32.548>
- [12] R. K. Gupta, W. Scheid and W. Greiner, Phys. Rev. Lett. **35**, 353 (1975).
<https://doi.org/10.1103/PhysRevLett.35.353>
- [13] G. Audi and A. H. Wapstra, Nucl. Phys. A **595**, 409 (1995).
[https://doi.org/10.1016/0375-9474\(95\)00445-9](https://doi.org/10.1016/0375-9474(95)00445-9)
- [14] P. Moller, J. R. Nix, W. D. Myers and W. J. Swiatecki, At. Nucl. Data Tables **59**, 185 (1995).
<https://doi.org/10.1006/adnd.1995.1002>
- [15] J. Blocki, J. Randrup, W. J. Swiatecki and C. F. Tsang, Annals of Physics **105**, 427 (1977).
[https://doi.org/10.1016/0003-4916\(77\)90249-4](https://doi.org/10.1016/0003-4916(77)90249-4)
- [16] W. Reisdorf, J. Phys. G.: Nucl. Part. Phys. **20**, 1297 (1994). <https://doi.org/10.1088/0954-3899/20/9/004>
- [17] W. D. Myers and W. J. Swiatecki Phys. Rev. C **62**, 044610 (2000).
<https://doi.org/10.1103/PhysRevC.62.044610>
- [18] A. Winther, Nucl. Phys. A **594**, 203 (1995).
[https://doi.org/10.1016/0375-9474\(95\)00374-A](https://doi.org/10.1016/0375-9474(95)00374-A)
- [19] R. K. Gupta et al., J. Phys. G. **31**, 631 (2005).
<https://doi.org/10.1088/0954-3899/31/7/009>
- [20] R. Kumar, Phys. Rev. C **86**, 044612 (2012).
<https://doi.org/10.1103/PhysRevC.86.044612>



Journal of Nuclear Physics, Material Sciences, Radiation and Applications

Chitkara University, Saraswati Kendra, SCO 160-161, Sector 9-C, Chandigarh, 160009, India

Volume 9, Issue 1

August 2021

ISSN 2321-8649

Copyright: [© 2021 Nitin Sharma and Manoj K. Sharma] This is an Open Access article published in Journal of Nuclear Physics, Material Sciences, Radiation and Applications (J. Nucl. Phy. Mat. Sci. Rad. A.) by Chitkara University Publications. It is published with a Creative Commons Attribution- CC-BY 4.0 International License. This license permits unrestricted use, distribution, and reproduction in any medium, provided the original author and source are credited.